International Journal on Advanced Science Engineering Information Technology

Vol.13 (2023) No. 3
ISSN: 2088-5334

Magnetic Signature and Element Content of Upflow and Outflow Hotspring in Arjuno–Welirang Geothermal System

Siti Zulaikah [a,*], Cathlea Syafiera Damayanti [a], Hafiz [b], Cahyo Aji Hapsoro [a], Yoyok Adisetio Laksono [a], Bambang Heru Iswanto [c], Jason Scott Herrin [d], Muhammad Fathur Rouf Hasan [e,f]

[a] *Department of Physics, Faculty of Mathematics and Natural Science, Universitas Negeri Malang, Malang, 65145, Indonesia*
[b] *Faculty of Mining and Petroleum Engineering, Institut Teknologi Bandung, Bandung, 40132, Indonesia*
[c] *Department of Physics, Faculty of Mathematics and Natural Science, Universitas Negeri Jakarta, Jakarta Timur, 13220, Indonesia*
[d] *Earth Observatory Singapore, Nanyang Technological University, 50 Nanyang Avenue, 639798, Singapore*
[e] *Department of Civil Engineering, Politeknik Negeri Jakarta, Depok, 16425, Indonesia*
[f] *Department of Physics, Universitas Brawijaya, Malang, 65145, Indonesia*
Corresponding author: [*]siti.zulaikah.fmipa@um.ac.id

***Abstract*— Research on magnetic properties and chemical element content of environmental deposits has been conducted for various purposes. This study focuses on characteristic magnetic susceptibility, magnetic mineral morphology, and the elemental composition of Cangar and Padusan hot springs in the Arjuno-Welirang geothermal system to differentiate upflow and outflow systems, respectively. The measurements were performed for better understand the relation between magnetic susceptibility, Fe-Silicate content, magnetic mineral morphology, surface temperature and compare these characteristics in two kinds of hot springs in the same mountain system. Magnetic susceptibility ranged (7.558 - 62.694) × 10^{-6} m^3/kg with an average of 30.651 × 10^{-6} m^3/kg for Cangar (upflow) and (11.821 - 28.101) × 10^{-6} m^3/kg with an average of 18.148 × 10^{-6} m^3/kg for Padusan (outflow). In situ magnetic minerals extracted of hot springs are averaged of magnetic susceptibility is 26.981 × 10^{-6} m^3/kg for Cangar and 24.445 × 10^{-6} m^3/kg for Padusan. The element content dominated by Al, Si, K, Ca, Ti and Fe, where Fe is more abundant in Cangar as an upflow. The higher magnetic susceptibility, the greater of Fe-silicate content in both of hot springs. The surface temperature ranged from 38 - 48°C, where the higher temperature, the magnetic susceptibility increased. In Cangar, extracted magnetic minerals tend show crystalline, especially hedralic shape with very fine surface, clean and free of impurities. Meanwhile, some magnetic minerals are also found in spherical shapes, especially in Padusan.**

***Keywords*— Magnetic susceptibility; element content; geothermal; upflow; outflow.**

Manuscript received 30 Jun. 2022; revised 18 Mar. 2023; accepted 7 May 2023. Date of publication 30 Jun. 2023.

I. INTRODUCTION

Indonesia's geothermal potential of around 28.91 GW is spread over 312 locations. Of the total geothermal potential, only about 5% has been explored. One of the geothermal spots that have not been explored is Arjuno Welirang [1]. Several studies have been carried out related to the geological, geophysical, and geochemical analysis of the Arjuno Welirang geothermal system [2] and potential energy analysis [3]. In this study, the magnetic properties of deposits in the geothermal area were tested to expand the application of the rock magnetism method as one of the signatures in the geothermal environment, especially as a differentiation clue of upflow and outflow, which in the future can use for maturity indicator or one of the characterization methods of geothermal reservoirs. This method will support the early methods such as gravity and magnetic [4]. Some gravity data of geothermal also accompanies geochemical analysis [5].

Rock magnetism methods have been widely used to evaluate environmental changes, such as evaluating polluted or non-polluted land with measured magnetic properties parameters such as magnetic susceptibility and supported by magnetic mineral morphology. Magnetic properties can even differentiate sources of pollutants in industrial areas [6]–[9]. Several studies have combined magnetic methods and geochemistry to describe the mapping of polluted areas due to heavy metal exposure, where heavy metal levels are measured by the high magnetic susceptibility and the presence of spherical grain of magnetic minerals [10]–[14]. Integrating magnetic and geochemical properties is also suitable for

tracing sources of pollution from Zinc [15] and Arsenic [16]. In this study, the magnetic susceptibility and element measurements were conducted to evaluate deposits at geothermal locations. Magnetic susceptibility can be useful during the initial stages of geothermal exploration in identifying hydrothermally altered rock and zones of hydrothermal alteration both at the surface and from drilled wells in a geothermal system. The study indicates a decrease in χ_{lf} values with depth in the two geothermal wells corresponding with: (1) an increase in the reservoir temperature and hydrothermal alteration and (2) a decrease in the concentration of Fe-Mg silicate and opaque minerals [17]. In this study, measurements of magnetic susceptibility and morphology of magnetic minerals, as well as geochemical tests conducted to identify the magnetic characteristics of the depositional environment in the form of hot springs with upflow and outflow characteristics.

Many geophysical methods have been applied for mapping and geothermal exploration, including the magnetic method [18]–[20]. A more detailed analysis of the magnetic characteristics and element content of material from geothermal areas can be conducted in the laboratory using physical methods. This study analyzed magnetic minerals and sediment samples in Padusan and Cangar hot springs, East Java, Indonesia. The magnetic properties can support or integrate with other geophysical methods [21].

II. Material and Method

A. Geology and Sampling Location

The Cangar and Padusan hot springs manifest the Arjuno-Welirang geothermal system with geographic coordinates 112°32'01.01" E and 7°44'31.80" S for Cangar and 112°32'59.57" E and 7°41'14.59" S for Padusan. The two hot springs are about 6 km apart. In general, this area consists of lava and pyroclastic flow. The bedrock of the two hot spring systems is the Qpva formation (Young Anjasmoro rock formation) which consists of volcanic breccia, tuff, and lava [22]. The Padusan hot spring is located in the area of andesite lava and pyroclastic rock, Mt Welirang products which are about 900 meters above sea level, while the Cangar hot spring is in the pyroclastic flow of Mt Kembar, which is about 1600 meters above sea levels. Based on the geochemical analysis, the reservoir temperature is estimated to be up to 175°C, and the temperature of the two hot springs is around 55°C [3]. In this study, the average temperature of the Cangar was 52°C with an air temperature of around 22°C, and the average temperature of the Padusan was around 48°C with an air temperature of 22 to 25°C.

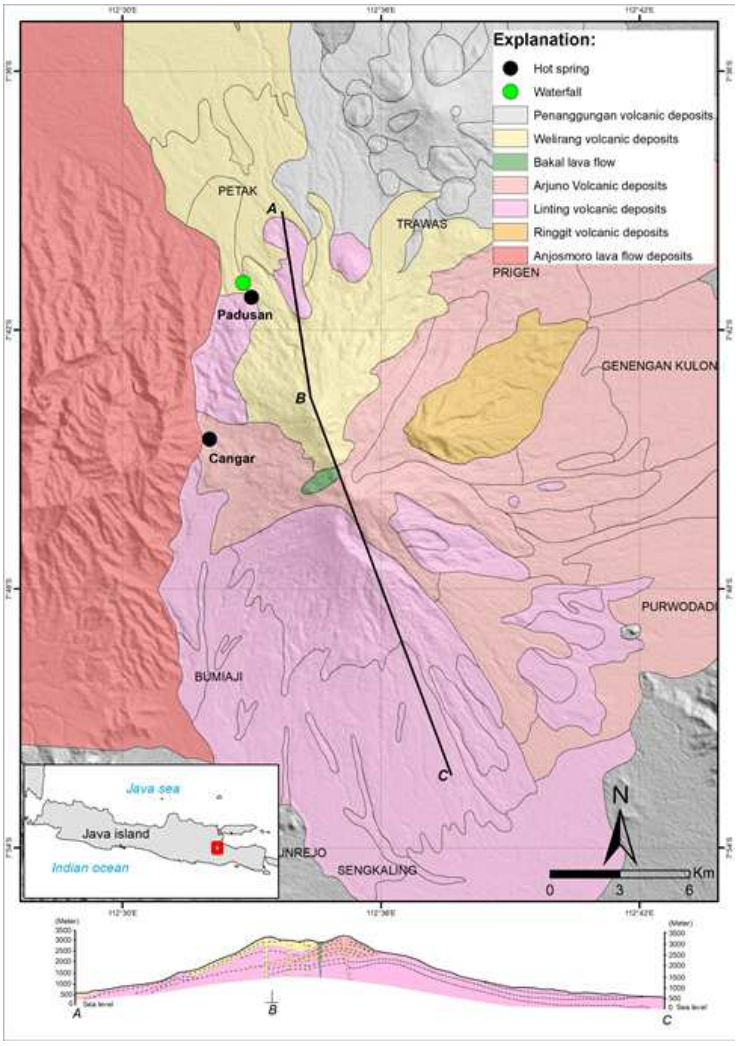

Fig. 1 Geological Map of Cangar Padusan. The Cangar hotspring is in the Arjuno Volcanic Deposits, while the Padusan Hotspring is in the Welirang and Linting Volcanic Deposits.

B. Cangar and Padusan Samples

The samples in this study consisted of deposits in hot springs, deposits in hot springs runoff, and in-situ extraction of magnetic minerals in both hot springs. Deposits samples in hot springs are marked with SE, in situ extracted magnetic minerals are marked with SM, and deposits samples in hot spring runoff are marked with C (Cangar) and P (Padusan). Likewise, the addition of C for Cangar and P for Padusan in SE and SM.

There are three springs in the Padusan area and one in the Cangar area. SE and SM were taken from the spring and its surroundings, while C and P were taken at 5 locations with a sampling point spacing of approximately 50 meters. For each hot spring, 50 samples were obtained, and 25 were selected to measure their magnetic susceptibility. Samples were taken from surface deposits in hot springs and hot springs runoff rivers. Samples were then put in a standard plastic sample holder for measuring magnetic susceptibility with a diameter of 2.1 cm and height of 2 cm. Magnetic susceptibility measurement was conducted using a magnetic susceptibility meter Bartington MS2B. Elemental content was measured using X-Ray Fluorescence (XRF). There were four samples of magnetic mineral extraction from C, and P tested for magnetic mineral morphology by SEM EDX.

III. Result and Discussion

The results of the elemental content test using XRF and the average magnetic susceptibility test are shown in Tables 1 and 2. Six dominant elements have magnitude above 1% of the measured sample. The elements are Al, Si, K, Ca, Ti, and Fe. Fe is the largest element, around 40-49%, followed by elements of Si, which is 18-23%. The details data is listed in Table 1..

TABLE I
CHEMICAL ELEMENTS CONTENT BASED ON XRF MEASUREMENTS OF CANGAR SAMPLES

Chemical Element	Sample C (Cangar)							
	SM 1.1	SM 1.2	SM 1.3	SE 1.1	SE 1.2	SE 1.3	SC 1.3	SC 2.3
Al	0	4	3.5	11	11	11	10	7.4
Si	9.76	11.3	9.93	28.4	27.9	26.8	21.8	23.3
K	0.52	0.62	0.53	3.13	2.86	2.66	2.03	2.59
Ca	2.14	2.79	2.16	11.9	11.8	11.8	10.1	14.6
Ti	5.33	5	5.15	2.1	2.12	2.14	2.49	1.64
V	0.52	0.47	0.49	0.1	0.11	0.11	0.2	0.10
Cr	0.09	0.09	0.09	0.07	0.07	0.08	0.07	0.085
Mn	0.58	0.61	0.72	0.89	1.1	0.92	1	0.77
Fe	78.6	73.4	75.7	39	39.3	40.8	48.5	40.2
Cu	0.076	-	-	0.17	0.17	0.17	0.19	0.14
Zn	0.07	0.06	0.06	0.04	0.02	0.03	0.08	0.08
Sr	-	-	-	0.86	0.76	0.85	0.6	0.86
Eu	0.67	0.65	0.6	0.64	0.68	0.72	0.5	-
Re	0.2	0.2	0.2	0.4	0.4	0.4	0.3	0.3
P	0.32	0.32	0.38	0.89	0.94	0.93	0.95	0.3
Ba	-	-	-	0.4	0.3	0.2	-	0.3
Rb	0.46	0.4	0.41	0.3	-	-	-	-
Bi	0.64	-	-	-	-	-	-	-
Br	-	-	-	-	-	-	-	-
Hg	-	-	-	-	-	-	-	-
Pb	-	-	-	-	-	-	-	-
S	-	-	-	-	-	-	0.96	-
Mo	-	-	-	-	-	-	-	6.65
Fe + Si	88.3	84.73	85.6	67.4	67.2	67.6	70.32	63.5
χ_{lf} ($\times 10^{-6}$ m^3/kg)	21.52	9.93	49.48	19.73	18.22	18.56	34	27

In some cases, the presence of Fe, Si and Mg elements can be used to indicate the presence of geothermal alteration and is associated with low-frequency magnetic susceptibility, as shown in the core sample of Los Azufres geothermal area [17]. In this study, there is no Mg element found. The relation between magnetic susceptibility and Fe-silicate is analyzed in the following discussion.

The elemental content of Ca in sediments runoff from hot springs is relatively high and, based on the geochemical analysis of geothermal water in both locations, shows that the elemental content of iron (Fe) and carbonate (Ca) in hot springs is also relatively high [3], thus allowing for the relatively high deposition of Fe and Ca deposits. Some samples of Padusan showed the presence of Pb and Hg content which is supposed by the anthropogenic input of pollutants.

The results of magnetic susceptibility measurements show that the magnetic susceptibility of magnetic mineral samples around the Cangar hot springs ranges from 9.933 to 49.488 $\times 10^{-6}$ m^3/kg with an average of 26.981×10^{-6} m^3/kg. Meanwhile, the deposits susceptibility found at the source point shows a range of 7.558 – 62.694×10^{-6} m^3/kg with an average of 30.651×10^{-6} m^3/kg. For Padusan, the magnetic mineral samples ranged from 14.300×10^{-6} m^3/kg to 31.906×10^{-6} m^3/kg, averaging 24.445×10^{-6} m^3/kg. For runoff deposits, 11.821 – 28.101×10^{-6} m^3/kg with an average of 18.148×10^{-6} m^3/kg. Based on the average of the magnetic susceptibility of the samples from the two places, it shows that Cangar is higher magnetic susceptibility than that Padusan.

This susceptibility is one order higher than the other deposits, such as the paddy soils in Malang and Madiun [23], and less than that of beach sand [24]. The high magnetic susceptibility is suspected that the magnetic minerals in the hot spring environment are dominated by lithogenic input, whereas the volcanic areas are the source of magnetic minerals commonly marked by magnetite and titanomagnetite.

TABLE II
CHEMICAL ELEMENTS CONTENT BASED ON XRF MEASUREMENTS OF PADUSAN SAMPLES

Chemical Element	Sample P (Padusan)						
	SM 1	SM 2	SM 3	SE 2	SE 3	SP 1.3	SP 5.2
Al	6	3.2	4.1	5.4	7.8	5.4	9
Si	7.2	11.9	11.2	19.7	23	18.7	22.7
K	0.29	0.63	0.44	1.8	2.17	1.91	2.3
Ca	1.66	10.1	2.97	33.2	27.5	16.2	11.5
Ti	6.18	4.84	5.67	1.4	1.54	2.04	2.42
V	0.54	0.43	0.46	0.097	0.093	0.15	0.16
Cr	0.12	0.097	0.094	0.071	0.079	0.083	0.081
Mn	0.52	0.61	0.56	0.6	0.58	0.76	1.1
Fe	75.09	65.27	72.16	34.8	29.3	44.0	47.57
Cu	0.057	0.07	0.068	0.11	0.12	0.12	0.19
Zn	0.1	0.12	0.08	0.03	0.01	0.04	0.06
Sr	-	-	-	0.75	0.62	0.68	0.85
Eu	0.63	0.58	0.58	0.4	0.3	0.5	0.6
Re	0.2	-	0.2	0.3	0.32	0.4	0.4
P	0.27	0.41	0.39	0.76	0.32	0.3	0.87
Ba	-	-	-	0.4	0.4	-	-
Rb	0.36	0.36	0.35	-	-	-	-
Bi	0.61	-	-	-	-	-	-
Br	0.25	-	-	-	-	-	-
Hg	-	0.44	0	0.2	-	-	-
Pb	-	0.88	-	-	-	-	-
S	-	-	0.6	-	-	1.4	-
Mo	-	-	-	-	5.9	7.2	-
Fe + Si	88.29	77.17	83.36	54.5	52.3	62.7	70.27
χ_{lf} ($\times 10^{-6}$ m^3/kg)	27.13	31.90	14.30	13.96	14.06	25	20

From the magnetic susceptibility range of the two hot springs, it shows that the susceptibility is consistent, it would be because the hot springs are located in the same mountain system, the Arjuno-Welirang system, with the same bedrock called the Young Anjasmoro rock formation, Qpva (Figure 1). The range of magnetic susceptibility is greater than the range with two cores in the Los Azufres geothermal area [17].

Samples from both hot springs contain 40-50% Fe and an exceptionally low sulfur content of about 1%. While the Ca content is around 10-15% and Si is around 20%. The Fe + Si elements combination is positively correlated with the low-frequency susceptibility value shown in Figure 2. The higher of Fe + Si content, the higher the magnetic susceptibility. The same result was reported by Pandarinath et al. (2014), who studied earlier core samples taken from a geothermal area. These results show the increase in Fe-Mg silicate is directly proportional to the value of χ_{lf} [17]. This study only uses Fe-Si without involving Mg because Mg elements were not found. The positive correlation of the addition of Fe-Si elements to the magnetic susceptibility illustrates that the bulk susceptibility of the sample is the total susceptibility of ferromagnetic, paramagnetic, and diamagnetic minerals, which is formulated by $\chi_t = \chi_f + \chi_a + \chi_p + \chi_d$, where Fe and Si are representative elements for ferromagnetic and diamagnetic minerals in significant amounts. This discovery also proposes a new proxy for tracing the specific geothermal environment, which is rich in Fe and Si element in tropical volcanic regions. Other unique parameters need more analysis.

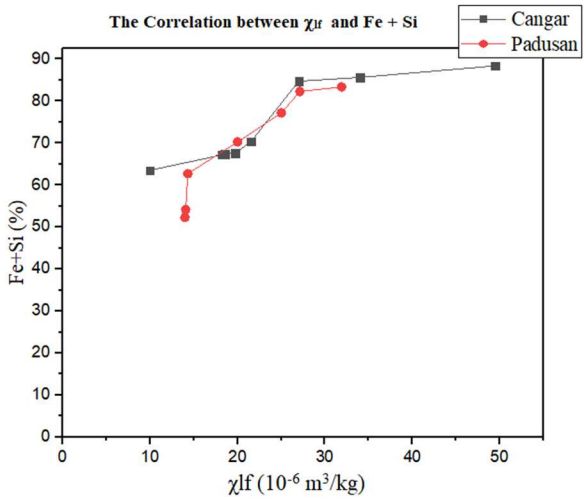

Fig. 2 The Correlation of Low frequency (χ_{lf}) magnetic susceptibility and Fe+Si

Dependence frequency magnetic susceptibility analysis on magnetic mineral samples extracted in situ at Cangar hot springs showed an average of 4.77% and for χ_{fd} deposits samples = 2.182%. For Padusan $\chi$the $_{fd}$ of magnetic mineral extraction in situ was 1.316%, and for a deposit χ_{fd} = 1.088%. From the results of the analysis based on Dearing (1999) [25], information was obtained that in the sample from Padusan, almost all grain sizes are in the multidomain (MD) range, while the sample from Cangar shows grain sizes with a wider

range from MD to a single domain (SD). The distribution of magnetic mineral domains illustrates in Figure 3. The graph's range is based on Dearing's method [25]. This grain size range analysis matches with 100x magnification SEM imaging data of magnetic grains extracted from the Padusan sample (P1.3 and P2.5), which tend to be abundant in the presence of large magnetic minerals with a size of about five hundred microns. Meanwhile, the SEM results for the extraction of grains from Cangar (C1.3 and C2.3) show that the presence of large magnetic grains is less. When the presence of large magnetic minerals decreases, it will be seen that the grain size estimation based on χ_{if} vs χ_{fd} is not dominated by large magnetic minerals or multidomain (MD), see Figure 4.

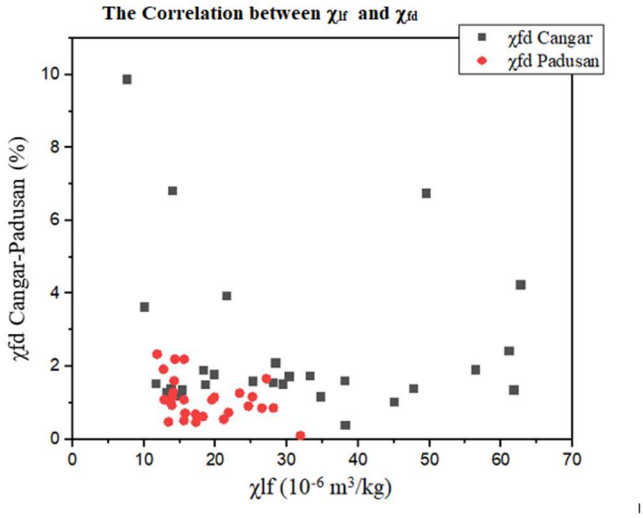

Fig. 3 Grain size distribution due to χ_{if} vs χ_{fd} based on Dearing's Method (1999)

The relation between the magnetic susceptibility of the sample and temperature shows that in the range of temperature 38 to 48 °C, the higher temperature would be the greater magnetic susceptibility value. In this range, the local temperature does not affect the susceptibility value. Still, the susceptibility value is more dominated by the presence of lithogenic minerals, where the grain size is larger, so the magnetic susceptibility of samples from Cangar is higher than Padusan. The description of the increased susceptibility and temperature of the two hot springs shows in Figure 4.

Regarding the flow characteristics, Cangar shows a measured temperature of 48°C, and Padusan, an outflow, indicates a lower temperature of around 43 °C. The Cangar samples show a larger χ_{fd} than Padusan, indicating that magnetic minerals are smaller than those of Padusan. Mixed and distributed from MD and SD. Hot water in the upflow system takes a longer or deeper path so that the magnetic minerals from the reservoir experience a decrease in size due to transportation to the surface and mixing with MD magnetic minerals that are already on the surface. Meanwhile, the outflow tends to show a magnetic mineral distribution that is multidomain (MD), which indicates the dominance of surface magnetic minerals and does not experience a long transport.

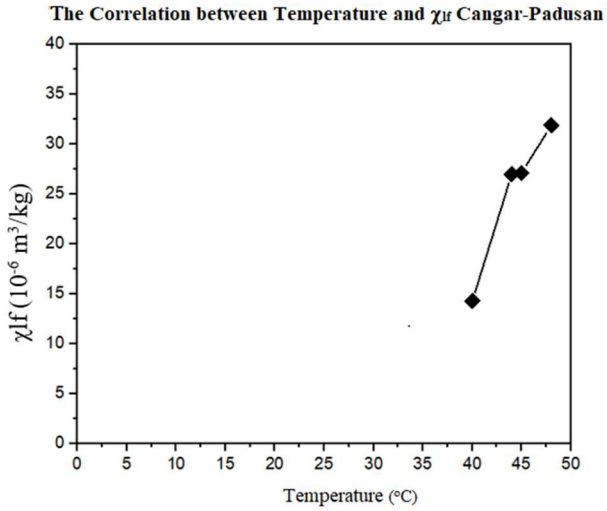

Fig. 4 Temperature vs χ_{lf}. Increase in temperature of hot springs in the range of 38 to 48 °C measured when sampling deposits and magnetic minerals in situ extractions. Magnetic susceptibility is the average of the entire sample at each location.

TABLE III
MAGNETIC CHARACTERISTICS AND ELEMENTAL CONTENT OF MAGNETIC MINERAL SAMPLES AND DEPOSITS AROUND CANGAR AND PADUSAN SOURCE POINTS

Parameters	Cangar		Padusan	
T_{ave}	48°C		43°C	
Fe_{ave}	57.81 %		55.324%	
Range of χ_{lf}	Magnetic Minerals	Deposit	Magnetic Minerals	Deposit
	(9.933– 49.488) $\times 10^{-6}$ m^3/kg	(7.558–62.694) $\times 10^{-6}$ m^3/kg	(14.300 – 31.906) $\times 10^{-6}$ m^3/kg	(11.821 –28.101) $\times 10^{-6}$ m^3/kg
$\chi_{lf\ ave}$	26.981× 10^{-6} m^3/kg	30.651× 10^{-6} m^3/kg	24.445× 10^{-6} m^3/kg	18.148× 10^{-6} m^3/kg
$\chi_{fd\ ave}$	4.77%	2.18%	1.32%	1.09%
Magnetic domain	From MD to SD		Most the samples MD	

Morphology of the magnetic minerals from extracted samples, in general, show a crystalline, spherical, and irregular shape with a smooth surface compared to other magnetic minerals extracted from deposits in other environments such as river sediments and lake or reservoir deposits (Fig. 5). The smooth surface of magnetic minerals P1.3 with magnification 500x and C 2.3 magnification 750x thought caused by the continuous flow of rivers with relatively high temperatures compared to other normal environments, which are generally around 23 °C. This condition could clean the impurities of magnetic minerals bearing and in the long period, would be smoother and grow round.

Some of the magnetic minerals suspected as Titanomagnetite with dominant element Fe-Ti-O-Al-Mg with Si 0.73 wt% (Fig 5d), Titanomagnetite with a dominant element contribution of Fe-Ti-O-Al-Mg and Si (3.53 Wt%) (Fig 5e). Titanomagnetite with dominant element Fe-Ti-O-

Al-Mg with Si 1.05 Wt% (Fig 5f). Spherulle magnetite Fe 84 Wt% and O 15 Wt% (Fig 5g). Magnetic minerals dominated by Fe-Ti-O-Al-Mg, where the Al-Mg is 2.42 Wt% and 1.91 Wt% with no Si (Fig 5h).

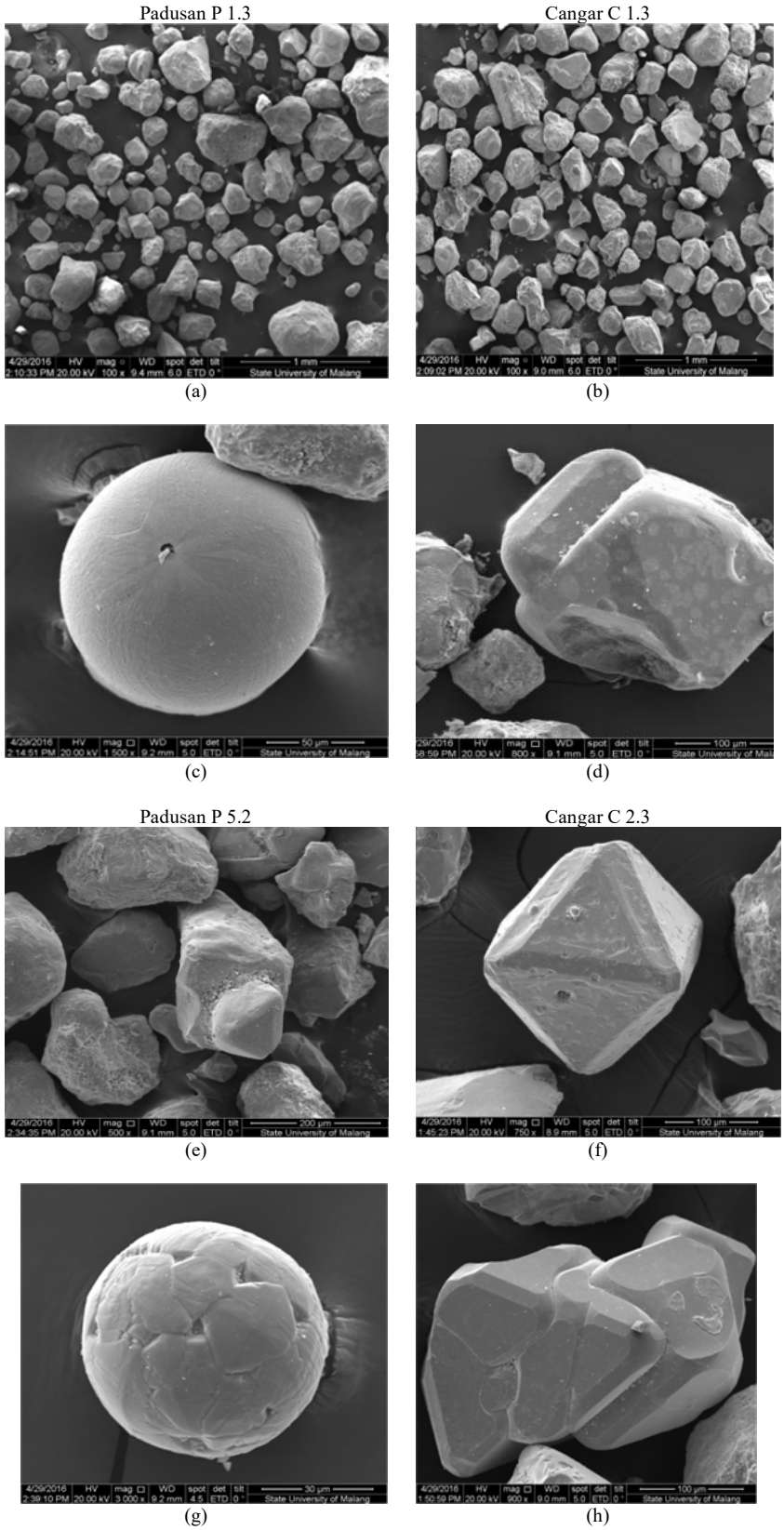

Fig. 5 SEM of magnetic mineral extraction from Padusan (left) and Cangar (right). The grain size distribution of magnetic minerals extracted from sample P1.3 with magnification in 100×(a) and C1.3. in 100×(b). Spherules magnetic minerals, showing surface 'orange peel' extracted from Padusan, 500×(c), Crystalline magnetic mineral from Cangar with magnification 800×(d), Crystalline magnetic mineral from Padusan with magnification in 500×(e), Magnetic mineral with crystalline shape and magnification 750×(f), Spherule magnetite from Padusan with magnification 2500×(g), Crystalline magnetic mineral with clean surface frrom Cangar with magnification 900×(h)

Several things related to the morphology of magnetic minerals as follows:

- Magnetic minerals are very clean both as individual or bearing compared to magnetic minerals extracted from other deposits, such as soil in agricultural or rivers environments that do not affected by hot water.
- Magnetic minerals that contributed by Fe-Ti-O-Mg-Al were cleaner or smoother than minerals contributed by Fe-Ti-O-Mg-Al with Si and Ca. Si and Ca are 'impurities;' elements in the presence of pure magnetite or titanomagnetite minerals. Mineral surfaces containing Si tend to be rough and partially porous. The more Si content is attached to the magnetic mineral, the surface of the magnetic mineral will be more rough or more porous, even with holes.
- The magnetic minerals are crystalline or spherules having a size of about 60 micron. This is in line with other magnetic spherules found in various deposits [24], and the shape of the spherule can indicate that the magnetic mineral originates from anthropogenic pollutants such as industrial or motor vehicles.

At 100× magnification, four samples extracted and analyzed showed that the extracted magnetic minerals tended to be clean and not has much impurity as is often found in other deposits. Extraction is also relatively easy. This condition is influenced by where the magnetic mineral deposition occurs in the hot water environment so that it can easily minimize organic impurities. Spherical magnetic minerals, especially those found in samples from Padusan, can be suspected of these magnetic minerals coming from the fly ash of motorized vehicles passing by around the hot springs. The spherical shape of these magnetic minerals is also commonly found in areas with high pollution levels where the spherical magnetic minerals result from industrial and transportation combustion [26], [27].

Spherical magnetic minerals are often found in the Padusan area due to the large amount of motor vehicle pollution that passes through the main road, which is only about 50 meters from the Padusan hot spring where the road is the main access for Padusan hot spring tourism. The area is also close to the home industry area. The alleged contribution of magnetic pollutants is also supported by XRF data which shows that several Padusan samples show the presence of Pb, Hg and Mo, which are usually released by motorized engines [28]. This condition is quite different from the Cangar hot springs, which are far from the highway or tourist parking area, so no magnetic mineral spherules are found in the Cangar sample, and perfect crystalline forms dominated magnetic minerals.

Based on previous research conducted by Sumartono [3], it was concluded that the Padusan hot springs originate from the outflow zone while the Cangar hot springs are in the upflow zone. The results of this study obtained data with two different spot: The Padusan hot spring has a lower temperature than Cangar, and the distribution of magnetic mineral domains is also wider for Cangar, suspected of having magnetic minerals originating from different depth sources and have long transport in the Cangar hot spring system. This condition allows the domain of the magnetic minerals to spread from MD to SD. Multidomain minerals dominate the magnetic minerals that come from the outflow zone, and the magnetic minerals from the upflow zone are considered multidomain to a single domain. The extraction of magnetic minerals shows spherules, which are thought to originate from motor vehicles and the home industry. This results would support the other characterization methods for identifying geothermal zone such as thermal infrared [29] and some environment differentiation tool [9],[30]–[34].

IV. Conclusion

Cangar and Padusan Hotspring which have an upflow and outflow characteristic, respectively, has Al, Si, K, Ca, Ti and Fe as dominant element content, which Fe is greater in Cangar (upflow) than that of Padusan (outflow). The presence of the element Ca in the sample in the volcanic area is quite large, due to the location is in subduction zone product. The average magnetic susceptibility and temperature of upflow are greater than outflow. The Fe+Si susceptibility relation between the two hot springs shows that the higher the Fe+Si element content, the greater the magnetic susceptibility. The relation between exposure and temperature of hot springs shows a temperature range of 38 to 48 ºC. The higher the temperature would be, the greater of magnetic susceptibility. The magnitude of magnetic susceptibility is controlled by the abundance of magnetic minerals and is dominated by the distribution of magnetic minerals with multi-domains. Magnetic minerals indicate the abundance of Fe from both sources in situ extraction samples from hot springs in both places. Based on the frequency dependence susceptibility, it shows that the magnetic mineral domains originating from the Padusan hot spring runoff tend to be multidomain (MD). In contrast, those originating from Cangar have magnetic domains spread from MD to SP, although the presence of SP grains is exceedingly minute. The distribution of magnetic mineral domains can be used as an indicator of the geothermal system uplow and outflow.

The morphology of magnetic minerals in both places was found to be in crystalline forms, which presumed that the presence of lithogenic magnetic minerals is still dominant. Magnetic grain surface tends to be smooth and clean. Some of the magnetic mineral grains combined with the elements Si and Ca show a rough surface. Some grains have a porous texture but tend to be smooth and clean. The corners of the crystal tend to be smooth and not sharp due to the continuous erosion of hot water. Several magnetic minerals are also found in a perfectly round shape, suspected to be the result of the contribution of pollutants around Padusan, where the location of Padusan hot spring is near the main road in the tourist area, where motorised vehicles pass through the road. The magnetic properties, element content and morphology of magnetic mineral studies are useful for distinguishing characteristics of hot springs in a geothermal area.

Acknowledgement

The authors are grateful to Universitas Negeri Malang for the grant of overseas partnership, with contract number: 5.3.UN32.14.1/LT/2021. The first author is the recipient of the grant. The authors are obliged to supporting team by M. Bagas Setya Rachman and Ghiffani and sampling process team by Meilinda and Halimatus for supporting the research in Central Laboratory of Universitas Negeri Malang and XRF and SEM EDX data collection.

REFERENCES

[1] N. A. Pambudi, "Geothermal power generation in Indonesia, a country within the ring of fire: Current status, future development and policy," *Renewable and Sustainable Energy Reviews.*, vol. 81, pp. 2893–2901, 2018, doi: 10.1016/j.rser.2017.06.096.

[2] Y. Daud *et al.*, "Resistivity characterization of the Arjuno-Welirang volcanic geothermal system (Indonesia) through 3-D Magnetotelluric inverse modeling," *Journal of Asian Earth Sciences.*, vol. 174, pp. 352–363, 2019, doi: 10.1016/J.JSEAES.2019.01.033.

[3] U. Sumotarto, "Geothermal energy potential of Arjuno and Welirang volcanoes area, East Java, Indonesia," *International Journal of Renewable Energy Research.*, vol. 8, no. 1, pp. 614–624, 2018, doi: 10.20508/IJRER.V8I1.6690.G7336.

[4] M. S. Rosid and C. Sibarani, "Reservoir identification at Dieng geothermal field using 3D inversion modeling of gravity data," *Journal of Physics: Conference Series.*, vol. 1816, p. 012083, 2021, doi: 10.1088/1742-6596/1816/1/012083.

[5] J. Nouraliee, D. Ebrahimi, A. Dashti, M. Gholami Korzani, and S. Sangin, "Appraising Mahallat Geothermal Region using thermal surveying data accompanied by the geological, geochemical and gravity analyses," *Scientific Reports.*, vol. 11, no. 1, pp. 1–14, 2021, doi: 10.1038/s41598-021-90866-4.

[6] A. C. Narayana, M. Ismaiel, and C. P. Priju, "An environmental magnetic record of heavy metal pollution in Vembanad lagoon, southwest coast of India," *Marine Pollution Bulletin.*, vol. 167, p. 112344, 2021, doi: 10.1016/J.MARPOLBUL.2021.112344.

[7] M. A. E. Chaparro *et al.*, "Magnetic parameters as proxies for anthropogenic pollution in water reservoir sediments from Mexico: An interdisciplinary approach," *Science of The Total Environment.*, vol. 700, p. 134343, 2020, doi: 10.1016/J.SCITOTENV.2019.134343.

[8] B. Wang, X. Zhang, Y. Zhao, M. Zhang, and J. Jia, "Spatial and Temporal Distribution of Pollution Based on Magnetic Analysis of Soil and Atmospheric Dustfall in Baiyin City, Northwestern China," *International Journal of Environmental Research and Public Health.*, vol. 18, no. 4, p. 1681, Feb. 2021, doi: 10.3390/IJERPH18041681.

[9] M. C. Sorrentino *et al.*, "Multi-elemental profile and enviromagnetic analysis of moss transplants exposed indoors and outdoors in Italy and Belgium," *Environmental Sciences Europe.*, vol. 289, p. 117871, 2021, doi: 10.1016/J.ENVPOL.2021.117871.

[10] I. Szczepaniak-Wnuk, B. Górka-Kostrubiec, S. Dytłow, P. Szwarczewski, P. Kwapuliński, and J. Karasiński, "Assessment of heavy metal pollution in Vistula river (Poland) sediments by using magnetic methods," *Environmental Science and Pollution Research.*, vol. 27, no. 19, pp. 24129–24144, 2020, doi: 10.1007/S11356-020-08608-4/TABLES/3.

[11] A. Vasiliev, S. Gorokhova, and M. Razinsky, "Technogenic Magnetic Particles in Soils and Ecological–Geochemical Assessment of the Soil Cover of an Industrial City in the Ural, Russia," *Geosciences*, vol. 10, no. 11, p. 443, 2020, doi: 10.3390/GEOSCIENCES10110443.

[12] B. Górka-Kostrubiec, T. Magiera, K. Dudzisz, S. Dytłow, M. Wawer, and A. Winkler, "Integrated Magnetic Analyses for the Discrimination of Urban and Industrial Dusts," *Minerals*, vol. 10, no. 12, p. 1056, 2020, doi: 10.3390/MIN10121056.

[13] L. Alfonsi, P. Macrì, and M. Nazzari, "Rock magnetic and micro-morphological analysis on snow deposits: recognition of anthropogenic origin of particulate matter in urban and wilderness areas (central Italy)," *Annals of Geophysics.*, vol. 64, no. 2, p. GM215, 2021, doi: 10.4401/AG-8515.

[14] T. Alokhina, "Magnetic particles in the sediments of the south Ukraine rivers as the marker of the technogenic impact on the hydroecosystems," *E3S Web of Conferences.*, vol. 234, p. 00048, 2021, doi: 10.1051/E3SCONF/202123400048.

[15] G. N. Salomão, D. de L. Farias, P. K. Sahoo, R. Dall'agnol, and D. Sarkar, "Integrated Geochemical Assessment of Soils and Stream Sediments to Evaluate Source-Sink Relationships and Background Variations in the Parauapebas River Basin, Eastern Amazon," *Soil Systems.*, vol. 5, no. 1, p. 21, 2021, doi: 10.3390/SOILSYSTEMS5010021.

[16] T. Ouyang *et al.*, "Magnetic response of Arsenic pollution in a slag covered soil profile close to an abandoned tungsten mine, southern China," *Scientific Reports.*, vol. 10, no. 1, pp. 1–8, 2020, doi: 10.1038/s41598-020-61411-6.

[17] K. Pandarinath, R. Shankar, E. Santoyo, S. B. Shetty, A. Y. García-Soto, and E. Gonzalez-Partida, "A rock magnetic fingerprint of hydrothermal alteration in volcanic rocks - An example from the Los Azufres Geothermal Field, Mexico," *Journal of South American Earth Sciences.*, vol. 91, pp. 260–271, 2019, doi: 10.1016/J.JSAMES.2019.02.018.

[18] K. L. Kapper *et al.*, "The use and misuse of magnetic methods to monitor environmental pollution in urban areas," *Boletín de la Sociedad Geológica Mexicana.*, vol. 72, no. 1, pp. 1–44, 2020, doi: 10.18268/BSGM2018V72N1A111219.

[19] X. Zhao, Z. Zeng, Y. Wu, R. He, Q. Wu, and S. Zhang, "Interpretation of gravity and magnetic data on the hot dry rocks (HDR) delineation for the enhanced geothermal system (EGS) in Gonghe town, China," *Environmental Earth Sciences.*, vol. 79, no. 16, pp. 1–13, 2020, doi: 10.1007/S12665-020-09134-9/METRICS.

[20] M. K. Johnson, *Paleomagnetic and Structural Analysis of Geothermal Drill Core from Akutan, Alaska*. Washington: Western Washington University, 2020.

[21] B. Wang, X. Zhang, C. Gu, M. Zhang, Y. Zhao, and J. Jia, "Magnetism and grain-size distribution of particles deposited on the surface of urban trees in Lanzhou City, Northwestern China," *International Journal of Environmental Research and Public Health.*, vol. 18, no. 22, p. 11964, 2021, doi: 10.3390/IJERPH182211964/S1.

[22] S. Santosa and S. Atmawinata, *Geological Map of The Kediri Quadrangle*. Bandung: Geological Research and Development Center, 1992.

[23] S. Zulaikah, H. A. Niarta, and J. S. Herrin, "Magnetic signature of paddy soil in Malang and Madiun East Java - Indonesia," *AIP Conference Proceedings.*, vol. 2251, no. 1, p. 020002, 2020, doi: 10.1063/5.0016516.

[24] S. Zulaikah, T. D. Arisanti, and M. B. S. Rahman, "The effect of magnetic mineral grain size on magnetic susceptibility and MDF of iron sand from Senggigi beach, West Lombok, West Nusa Tenggara province of Indonesia," *AIP Conference Proceedings.*, vol. 2634, no. 1, p. 020026, 2023, doi: 10.1063/5.0113912.

[25] J. Dearing, *Environmental magnetic susceptibility : using the Bartington MS2 system*. London: British Library London, 1999.

[26] N. Jordanova, D. Jordanova, E. Tcherkezova, B. Georgieva, and D. Ishlyamski, "Advanced mineral magnetic and geochemical investigations of road dusts for assessment of pollution in urban areas near the largest copper smelter in SE Europe," *Science of The Total Environment.*, vol. 792, p. 148402, 2021, doi: 10.1016/J.SCITOTENV.2021.148402.

[27] K. S. Essa, S. Mehanee, and M. Elhussein, "Magnetic Data Profiles Interpretation for Mineralized Buried Structures Identification Applying the Variance Analysis Method," *Pure and Applied Geophysics.*, vol. 178, no. 3, pp. 973–993, 2021, doi: 10.1007/S00024-020-02553-6/METRICS.

[28] H. Huang, J. Zhang, H. Hu, S. Kong, S. Qi, and X. Liu, "On-road emissions of fine particles and associated chemical components from motor vehicles in Wuhan, China," *Environmental Research.*, vol. 210, p. 112900, 2022, doi: 10.1016/J.ENVRES.2022.112900.

[29] W. Cao *et al.*, "Identifying Upflow Zone Based on Thermal Infrared (TIR) Sensor and Field Measurements at Volcanic Field," *IOP Conference Series: Earth and Environmental Science.*, vol. 417, p. 012011, 2020, doi: 10.1088/1755-1315/417/1/012011.

[30] E. Petrovský, A. Kapička, H. Grison, B. Kotlík, and H. Miturová, "Negative correlation between concentration of iron oxides and particulate matter in atmospheric dust: case study at industrial site during smoggy period," *Environmental Sciences Europe.*, vol. 32, no. 1, p. 134, 2020, doi: 10.1186/S12302-020-00420-8/FIGURES/5.

[31] H. Chen, D. sheng Xia, B. Wang, H. Liu, and X. Ma, "Pollution monitoring using the leaf-deposited particulates and magnetism of the leaves of 23 plant species in a semi-arid city, Northwest China," *Environmental Science and Pollution Research*, vol. 29, no. 23, pp. 34898–34911, 2022, doi: 10.1007/S11356-021-16686-1/METRICS.

[32] C. S. Damayanti *et al.*, "Analysis of magnetic susceptibility and chemical elements of hot spring sediment in Tiris Village, Probolinggo Regency," *AIP Conference Proceedings.*, 2023, p. 020092, doi: 10.1063/5.0113958.

[33] K. Pandarinath, J. L. Rivas-Hernández, J. A. Arriaga-Fuentes, D. Yáñez-Dávila, E. González-Partida, and E. Santoyo, "Hydrothermal alteration of surficial rocks at Los Humeros geothermal field, Mexico: a magnetic susceptibility approach," *Arabian Journal of Geosciences.*, vol. 16, no. 4, pp. 1–15, 2023, doi: 10.1007/S12517-023-11306-3.

[34] L. M. Weydt, K. Bär, and I. Sass, "Petrophysical characterization of the Los Humeros geothermal field (Mexico): from outcrop to parametrization of a 3D geological model," *Geothermal Energy.*, vol. 10, no. 1, pp. 1–48, 2022, doi: 10.1186/S40517-022-00212-8.